precipitate was dissolved in toluene (20 mL) at 50 °C under nitrogen. Hexane was added to the red solution (ca. 20 mL), and the resulting solution was filtered and cooled at −15 °C. Red crystals were obtained over a period of 2 weeks: total yield ca. 20%. Anal. Calcd for $C_{72}H_{64}N_2P_4Ru_2$: C, 69.0; H, 5.5; N, 2.0; P, 8.1. Found: C, 68.2; H,5.2; N, 2.0; P,8.1.

Crystallographic Study. Owing to its air sensitivity, the crystal of $Ru_2N_2H_4(PPh_3)_4$ chosen for the study was protected by a Lindemann capillary.

Preliminary photographic studies with Weissenberg and precession cameras showed that the compound crystallizes in a monoclinic system. The observed systematic absences ($h0l$, $h + l = 2n + 1$; $0k0$, $k = 2n + 1$) are consistent with the $P2_1/n$ space group.

The setting angles of 25 hkl reflections, regularly distributed in the half sphere, automatically centered on a Enraf-Nonious CAD4 diffractometer, were used in a least-squares calculation which led to the cell constants (Table V). On the assumption of four formula units per cell, the calculated density $\rho_{calcd} = 1.30$ g·cm^{-3} was found to be of the order of magnitude for that type of compound. Owing to the instability of the compound, we were not able to get a value for ρ_{exptl}.

Data Collection. Table V gives pertinent details concerning the experimental data collection conditions. Reflections have been recorded in three shells with the same crystal. No significantly deviation from the average value of any of the intensity control reflections was observed. Data were thus processed in the usual way[27] using a value of 0.02 for p.

Structure Determination and Refinement. The structure has been solved by standard Patterson and Fourier methods with the help of the SHELX program.[28] Conditions of refinement and used agreement indices, R and R_w, are defined in Table V. Values of the atomic scattering factors and the anomalous terms used for P, N, C, and H are those included in the SHELX program. For Ru, they come from the ref 29.

From the Patterson function, the two Ru atoms were located, and on a subsequent Fourier map, the four phosphorus and 10 carbon atoms were found (C(1), C(2), C(3), C(5), C(6), C(7), C(8), C(13), C(14), and C(15)). Alternation of full-matrix least-squares refinements of isotropic atoms and difference Fourier maps then led to the location of all non-hydrogen atoms. At that point, two supplementary cycles of full-matrix least-squares refinements of the position of the Ru and P atoms (anisotropic), N (isotropic), and carbon atoms (isotropic) as phenyl rigid groups led to $R = R_w = 8.6\%$. Further refinements with introduction of all the hydrogen atoms of the 12 phenyl groups (as rigid group atoms with a fixed U_{iso} equal to the U_{iso} of the carbon bearing atom) led to $R = 8.3\%$ and $R_w = 7.5\%$ with a weighting scheme of the type $w = k/\sigma^2(F)$ ($k = 1.454$; 217 parameters). Any further attempt to improve the resolution failed probably due to the smallness and poor quality of the crystal (lack of intense reflections). A subsequent difference Fourier map did not permit a reliable location of the hydrido atoms. One of the phenyl groups presents rather high U_{iso} thermal parameters, which is probably the sign of a slight disorder, but we were not able to solve it.

Registry No. 1, 97570-08-6; 2, 87800-34-8; 3, 97570-07-5; 4, 97570-10-0; 5, 97570-09-7; 6, 97570-11-1; $Ru(C_8H_8)_2(PPh_3)_2$, 68088-93-7.

Supplementary Material Available: Tables of final anisotropic thermal parameters (Å × 10^2) with estimated standard deviations in parentheses, atomic positional and thermal parameters for hydrogen, and structure factors (16 pages). Ordering information is given on any current masthead page.

(27) Mosset, A.; Bonnet, J.-J.; Galy, J. *Acta Crystallogr., Sect. B: Struct. Crystallogr. Cryst. Chem.* **1977**, *B33*, 2639.
(28) Sheldrick, G. M. "SHELX-76, A Computer Program for Crystal Structure Determination"; University of Cambridge: Cambridge, 1976.
(29) "International Tables for X-Ray Crystallography"; Kynoch Press: Birminham, England 1975; Vol. IV, Tables 2.2A and 2.3.1.
(30) Pavel, N. V.; Quagliata, C.; Scarcelli, N. *Z. Kristallogr.* **1976**, *144*, 64.
(31) Calascibetta, F. G.; Bentini, M.; de Santis, P.; Morosetti, S. *Biopolymers* **1975**, *14*, 1667.

Asymmetric Catalyses. 16. Catalysts (cod)RhNN′ and [(cod)RhNN″]PF_6 (NN′ and NN″ = Optically Active Pyrrole and Pyridine Imines)[1]

Henri Brunner,* Peter Beier, and Georg Riepl

Institut für Anorganische Chemie, Universität Regensburg, D-8400 Regensburg, Germany

Ivan Bernal* and George M. Reisner

Department of Chemistry, University of Houston, Houston, Texas 77004, USA

Reinhard Benn and Anna Rufińska

Max-Planck-Institut für Kohlenforschung, Kaiser-Wilhelm-Platz 1, 4330 Mülheim a. d. Ruhr, Germany

Received October 4, 1984

A single-crystal X-ray analysis of [(cod)RhNN″]PF_6, **2**, was carried out, NN″ = Schiff base derived from 2-pyridinealdehyde and (*S*)-1-phenylethylamine. The solution conformations of **2** and complexes **1** and **3**, containing the corresponding pyrrole imine ligand, were determined by ^{1}H NMR NOE difference spectroscopy. The arrangement of the chiral N-substituent C*HMePh with respect to chelate ring and Rh coordination plane is compared with that of compounds studied previously. Good agreement is found between solid-state and solution conformations.

In the enantioselective hydrosilylation of ketones, rhodium(I) complexes of optically active pyrrole and pyridine imines of type **1–3** give optical inductions superior to those obtained with optically active phosphanes, the ligands usually used in asymmetric catalysis.[1,2] These imine and phosphane ligands differ in the way chirality is transmitted to the metal sites, where the prochiral substrates are transformed into the chiral products.[3,4]

(1) Asymmetric Catalysis, Part 15: Brunner, H.; Becker, R. *Angew. Chem.* **1984**, *96*, 221; *Angew. Chem., Int. Ed. Engl.* **1984**, *23*, 222.
(2) Brunner, H.; Riepl, G. *Angew. Chem.* **1982**, *94*, 369; *Angew. Chem., Int. Ed. Engl.* **1982**, *21*, 377; *Angew. Chem. Suppl.* **1982**, 769.

0276-7333/85/2304-1732$01.50/0

Scheme I

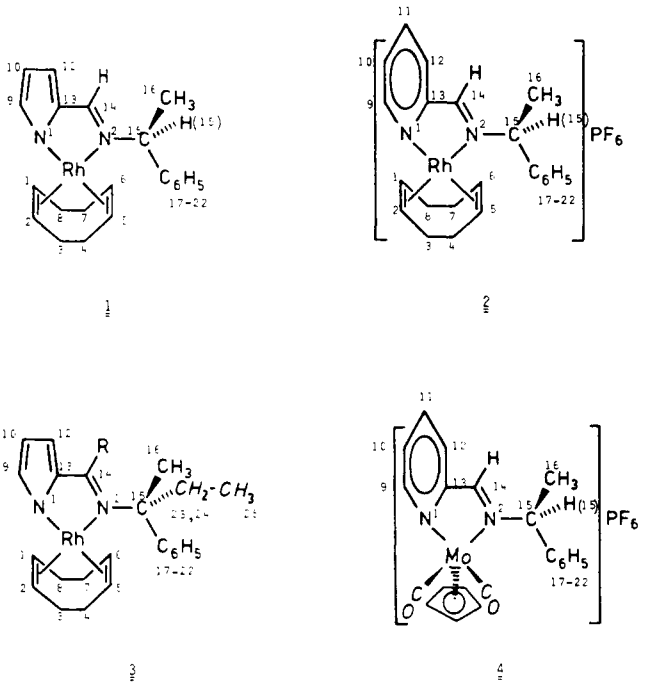

In the phosphane ligands the chiral information, located mostly on the chelate backbone, is transmitted by the chiral arrangement of the two phenyl rings of $P(C_6H_5)_2$ groups, the P atoms of which are coordinated.[5,6] The optical activity of the pyrrole and pyridine imine ligands in **1–3** is situated at the imine N substituent R*, derived from an optically active primary amine. On coordination, the lateral asymmetric substituent R* directly interacts with the adjacent metal positions.[1,7] It is this direct vs. the indirect interaction of a given chiral information with the metal coordination sites to which the superiority of the pyrrole and pyridine imine ligands in **1–3**, with respect to chelate phosphane ligands, is attributed.[3]

A series of conformational analyses of $C_5H_5(CO)_2Mo$ thioamidato and amidinato compounds showed that lateral asymmetric substituents R* at coordinated N atoms, in spite of free rotation about the N–R* bond, adopt specific conformations, controlled by interactions with substituents at the Mo atom as well as at the chelate ring.[8–16] Since in these systems C_5H_5/phenyl and C_5H_5/alkyl interactions play a major role, the results cannot be directly transferred to the hydrosilylation catalysts **1–3**. Therefore, a conformational analysis with **1–3** was carried out on the basis of X-ray structure analyses and NOE difference spectroscopy. Knowledge of the conformation of R* with respect to the chelate ring RhNCCN and the other coordination sites at the Rh atom is a prerequisite for improving the differentiation between *re*/*si* coordination of prochiral substrates and for predicting the correct absolute configuration of the products.

The results of the single-crystal X-ray structure determination of **2** are presented and compared with those of **1**, published previously.[17] The solution behavior of **1–3** is elucidated on the basis of 400-MHz ^1H NMR spectra, ^{13}C NMR spectra, variable-temperature measurements, and a detailed NOE difference spectroscopic study of **1** and **3** (Scheme I).

Table I. Summary of Data Collection and Processing Parameters (Complex 2)

space group	$P2_12_12_1$
cell constants	
a, Å	10.151 (6)
b, Å	10.277 (6)
c, Å	22.26 (1)
V, Å^3	2322.3
mol formula	$C_{22}H_{26}N_2PF_6Rh$
mol wt	566.33
molecules/unit cell	4
d (measd, flotation), g·cm^{-3}	1.61
d (calcd), g·cm^{-3}	1.62
abs coeff, cm^{-1}	8.00
radiatn (Mo Kα), λ, Å	0.710 73
data collection range	$4° \leq 2\theta \leq 60°$
scan width	$\Delta\theta = (1.00 + 0.35 \tan \theta)°$
max scan time, s	240
scan speed range, deg m^{-1}	0.4–5
total data collected	3829
data with $I > 3\sigma(I)$	1758
total variables	290
$R = \sum\|\|F_o\| - \|F_c\|\|/\sum\|F_o\|$	0.050
$R_w = [\sum w(\|F_o\| - \|F_c\|)^2/\sum w[F_o^2]^{1/2}$	0.046
weights	$w = \sigma(F_o)^{-2}$

Experimental Section

Complex **3** was prepared according to the procedures reported for complexes **1** and **2**.[18,19] For the synthesis of **1** and **2** optically pure imine ligands were used, whereas complex **3** was synthesized by using a racemic pyrrole imine ligand.

The 2-phenyl-2-aminobutane, needed for the preparation of the pyrrole imine ligand for complex **3**, was prepared by a Ritter reaction starting from 2-phenylbutanol-2,[20,21] which was obtained from a Grignard reaction of phenylmagnesium bromide and methyl ethyl ketone.

Crystals suitable for X-ray structure analysis were obtained by crystallizing a sample of **2**[18,19] from CH_2Cl_2/CH_3OH (1:2); red plates (0.5 × 0.5 × 0.3 mm).

The NMR spectra of **1–3** were measured by using a Bruker WH 400 spectrometer, equipped with an Aspect 2000 computer, with a fast pulse programmer and a CDC 96 double-drive disk. The ^1H NMR spectra of **1–3** were recorded at 400 MHz in 5-mm sample tubes at temperatures between 300 and 173 K. Nuclear Overhauser difference spectra were obtained under temperature control by using a technique described earlier.[22,23] The carbon-13

(3) Brunner, H. *Angew. Chem.* **1983**, *95*, 921; *Angew. Chem., Int. Ed. Engl.* **1983**, *22*, 897.
(4) Kagan, H. B. "Comprehensive Organometallic Chemistry"; Wilkinson, G., Stone, F. G. A., Abel, E. W., Eds.; Pergamon Press: New York, 1982; Vol. 8, p 463.
(5) Knowles, W. S.; Vineyard, B. D.; Sabacky, M. J.; Stults, B. R. "Fundamental Research in Homogeneous Catalysis"; Tsutsui, M., Ed.; Plenum Press: New York, 1979; Vol. 3, p 537.
(6) Vineyard, B. D.; Knowles, W. S.; Sabacky, M. J.; Bachmann, G. L.; Weinkauff, D. J. *J. Am. Chem. Soc.* **1977**, *99*, 5946.
(7) Brunner, H.; Rahman, A. F. M. M. *Z. Naturforsch., B: Anorg. Chem., Org. Chem.* **1983**, *38B*, 1332.
(8) Brunner, H.; Agrifoglio, G.; Benn, R.; Rufińska, A. *J. Organomet. Chem.* **1981**, *217*, 365.
(9) Brunner, H.; Agrifoglio, G. *J. Organomet. Chem.* **1980**, *202*, C43.
(10) Brunner, H.; Rastogi, D. K. *Bull. Soc. Chim. Belg.* **1980**, *89*, 883.
(11) Brunner, H.; Muschiol, M.; Bernal, I.; Reisner, G. M. *J. Organomet. Chem.* **1980**, *198*, 169.
(12) Bernal, I.; Creswick, M.; Brunner, H.; Agrifoglio, G. *J. Organomet. Chem.* **1980**, *198*, C4.
(13) Brunner, H.; Lukassek, J.; Agrifoglio, G. *J. Organomet. Chem.* **1980**, *195*, 63.
(14) Brunner, H.; Agrifoglio, G.; Bernal, I.; Creswick, M. *Angew. Chem.* **1980**, *92*, 645; *Angew. Chem., Int. Ed. Engl.* **1980**, *19*, 641.
(15) Brunner, H.; Rastogi, D. K. *Inorg. Chem.* **1980**, *19*, 891.
(16) Brunner, H.; Lukas, R. *Chem. Ber.* **1979**, *112*, 2528.
(17) Brunner, H.; Riepl, G.; Bernal, I.; Ries, W. H. *Inorg. Chim. Acta*, in press.
(18) Zassinovich, G.; Camus, A.; Mestroni, G. *J. Organomet. Chem.* **1977**, *133*, 377.
(19) Brunner, H.; Reiter, B.; Riepl, G. *Chem. Ber.* **1984**, *117*, 1330.
(20) Haaf, W. *Chem. Ber.* **1963**, *96*, 3359.
(21) Kosower, E. M.; Savern, D. J. *Tetrahedron Lett.* **1966**, 3125.

Table II. Atomic Coordinates and Thermal Parameters (×10³; H, ×10²; Rh, ×10⁴) (Complex 2)

atom	*x/a*	*y/b*	*z/c*	*U*(11)	*U*(22)	*U*(33)	*U*(12)	*U*(13)	*U*(23)
Rh	−0.04335 (13)	−0.18721 (11)	−0.11325 (5)	506 (6)	336 (5)	400 (5)	−56 (3)	15 (8)	−47 (7)
N2	−0.0306 (14)	−0.3641 (10)	−0.1589 (5)	43 (7)	44 (7)	38 (6)	−7 (5)	−3 (7)	−8 (5)
C1	−0.0357 (20)	0.0234 (12)	−0.977 (8)	68 (11)	32 (8)	92 (14)	6 (10)	16 (13)	−16 (8)
C2	−0.0383 (22)	−0.0405 (16)	−0.0423 (8)	91 (14)	78 (12)	73 (12)	−2 (15)	−15 (15)	−47 (11)
C3	−0.1515 (23)	−0.0607 (25)	−0.0023 (8)	145 (22)	205 (26)	51 (13)	−23 (21)	41 (15)	−56 (15)
C4	−0.2580 (21)	−0.1423 (18)	−0.0204 (7)	139 (19)	114 (18)	61 (12)	−70 (16)	51 (13)	−35 (12)
C5	−0.2396 (14)	−0.2076 (14)	−0.811 (7)	59 (10)	33 (10)	83 (13)	−11 (9)	27 (10)	−12 (9)
C6	−0.2403 (14)	−0.1419 (15)	−0.1331 (8)	38 (10)	37 (10)	75 (14)	−14 (9)	12 (9)	−9 (9)
C7	−0.2655 (22)	0.0013 (18)	−0.1411 (9)	83 (15)	59 (11)	144 (19)	3 (11)	−40 (14)	17 (12)
C8	−0.1586 (17)	0.0523 (16)	−0.1250 (11)	64 (13)	63 (13)	147 (20)	−11 (12)	7 (15)	11 (15)
N1	0.1587 (12)	−0.1959 (14)	−0.1300 (5)	57 (9)	46 (9)	55 (10)	−7 (9)	−9 (7)	−8 (6)
C9	0.2535 (15)	−0.1195 (14)	−0.1132 (9)	41 (10)	39 (9)	97 (13)	−1 (8)	11 (12)	−6 (12)
C10	0.3868 (20)	−0.1329 (20)	−0.1304 (10)	49 (13)	78 (15)	113 (18)	−26 (11)	−23 (12)	36 (13)
C11	0.4206 (18)	−0.2413 (20)	−0.1678 (10)	53 (13)	77 (13)	115 (16)	1 (11)	5 (12)	15 (12)
C12	0.3212 (18)	−0.3187 (18)	−0.1817 (9)	50 (10)	56 (11)	92 (13)	19 (13)	−6 (10)	−24 (14)
C13	0.1962 (14)	−0.3050 (18)	−0.1626 (6)	40 (9)	60 (10)	43 (9)	−11 (11)	11 (7)	16 (10)
C14	0.0878 (17)	−0.3900 (15)	−0.1768 (7)	64 (12)	22 (8)	35 (10)	2 (8)	4 (8)	−5 (7)
C15	−0.1381 (14)	−0.4601 (14)	−0.1710 (7)	42 (10)	28 (8)	54 (10)	−9 (8)	−18 (8)	−10 (8)
C16	−0.1115 (20)	−0.5597 (21)	−0.2207 (8)	77 (14)	85 (16)	36 (10)	−27 (12)	4 (11)	−16 (10)
C17	−0.1715 (15)	−0.5300 (12)	−0.1145 (8)	58 (10)	26 (7)	62 (10)	−1 (7)	15 (12)	−20 (9)
C18	−0.3027 (13)	−0.5707 (14)	−0.1074 (9)	26 (8)	96 (13)	99 (14)	−16 (9)	0 (10)	75 (13)
C19	−0.3325 (19)	−0.6340 (15)	−0.0532 (9)	77 (14)	58 (12)	110 (16)	−3 (11)	41 (13)	−29 (12)
C20	−0.2461 (21)	−0.6549 (15)	−0.0099 (7)	104 (17)	33 (10)	48 (11)	0 (11)	21 (11)	1 (8)
C21	−0.1223 (21)	−0.6225 (17)	−0.0167 (8)	110 (18)	68 (13)	57 (13)	−8 (13)	−1 (12)	3 (10)
C22	−0.0808 (15)	−0.5553 (13)	−0.0681 (7)	47 (12)	47 (9)	67 (11)	−12 (9)	−14 (9)	3 (9)
P	−0.6717 (6)	0.2654 (4)	−0.1778 (2)	108 (4)	50 (3)	59 (3)	−10 (3)	0 (3)	1 (2)
F1	−0.5789 (14)	0.1927 (14)	−0.1340 (5)	166 (5)					
F2	−0.7703 (12)	0.3392 (13)	−0.2215 (6)	144 (5)					
F3	−0.6991 (13)	0.3718 (12)	−0.1271 (6)	152 (5)					
F4	−0.6407 (10)	0.1635 (11)	−0.2280 (4)	107 (4)					
F5	−0.7862 (15)	0.1823 (16)	−0.1527 (7)	189 (6)					
F6	−0.5591 (15)	0.3504 (14)	−0.2026 (6)	180 (5)					

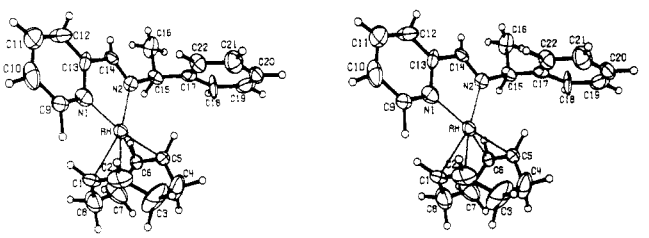

Figure 1. Stereoscopic view of the cation of **2** showing the atomic numbering system. The labeling of the hydrogens is such that their numbers are identical with those of the carbons they are attached to.

spectra were measured at 100.6 MHz by using 5-mm proton sample tubes at temperatures between 310 and 193 K. Gated spectra could be recorded for **1** and **2**; however due to concentrations of less than 1% only broad-band-decoupled spectra could be obtained for **3**. The assignment of the carbon resonances is based on reference data for chemical shifts,[24,25] coupling constants, and multiplicities.

X-ray Structure Determination of 2. Intensity measurements were carried out by using an Enraf-Nonius CAD-4 computer-controlled diffractometer. A summary of the crystallographically important parameters for data collection and processing is given in Table I. Accurate cell constants were determined from 25 strong, high angle reflections. The intensities were measured by using the θ–2θ scan technique, with the scan rate depending on the net count obtained in rapid prescans of each reflection. The standard reflections, monitored every 2 h, did not show any significant deviations from the initial measurements. In reducing the data, Lorentz and polarization factors were applied, but no absorption corrections were made. Standard deviations on the measured intensities were estimated by using Poisson's statistics. All data processing and calculations were carried out by using the SHELX 76[26] system of programs. The

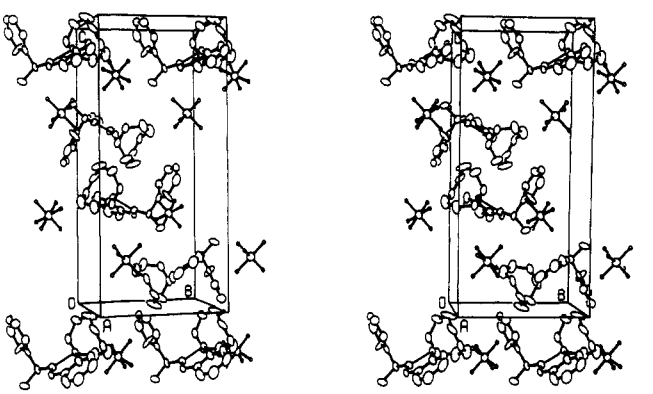

Figure 2. Stereoscopic view of the molecular packing of **2**. The hydrogen atoms were omitted for clarity.

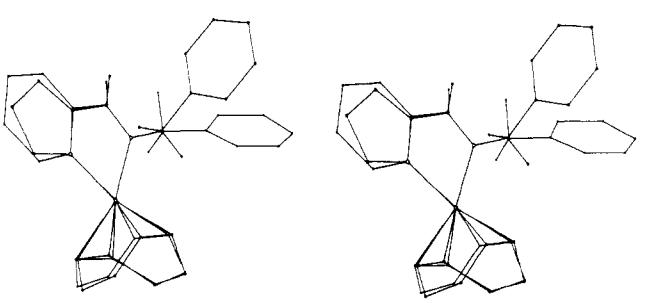

Figure 3. A double stereo picture of compounds **1** and **2**. Hydrogens, except for those attached to C14 and C15, were omitted for clarity.

(22) Benn, R.; Rufińska, A.; Schroth, G. *J. Organomet. Chem.* **1981**, *217*, 91.
(23) Benn, R.; Klein, J.; Rufińska, A.; Schroth, G. *Z. Naturforsch., B: Anorg. Chem., Org. Chem.* **1981**, *36B*, 1595.
(24) Bremser, W.; Franke, B.; Wagner, H. "Chemical Shift Ranges in Carbon-13 NMR Spectroscopy"; Verlag Chemie: Weinheim/Bergstr., West Germany 1982.
(25) Mann, B. E.; Taylor, B. F. "^{13}C NMR Data for Organometallic Compounds"; Academic Press: New York, 1981.
(26) Sheldrick, G. M. "SHELX-76 Programs for Crystal Structure Determination", University of Cambridge, 1979.

Table III. Intramolecular Bond Distances (Å) in 2

Rh–N1	2.086 (11)	C12–C13	1.35 (2)
Rh–N2	2.086 (9)	C13–C14	1.44 (2)
Rh–C1	2.19 (1)	N2–C14	1.29 (2)
Rh–C2	2.18 (1)	N2–C15	1.50 (1)
Rh–C5	2.13 (1)	C15–C16	1.53 (2)
Rh–C6	2.10 (1)	C15–C17	1.49 (2)
C1–C2	1.40 (2)	C17–C18	1.40 (2)
C2–C3	1.47 (2)	C18–C19	1.40 (2)
C3–C4	1.42 (2)	C20–C21	1.31 (2)
C4–C5	1.52 (2)	C21–C22	1.40 (2)
C5–C6	1.34 (2)	C22–C17	1.41 (2)
C6–C7	1.50 (2)	P–F1	1.55 (1)
C7–C8	1.41 (2)	P–F2	1.59 (1)
C8–C1	1.51 (2)	P–F3	1.60 (1)
N1–C9	1.30 (2)	P–F4	1.56 (1)
N1–C13	1.39 (2)	P–F5	1.55 (1)
C9–C10	1.41 (2)	P–F6	1.54 (1)
C10–C11	1.43 (2)	Rh–Cen1[a]	2.07 (1)
C11–C12	1.32 (2)	Rh–Cen2[a]	2.00 (1)
		F4···H15	2.42 (4)

[a] Cen1 and Cen2 refer to the geometric centers of the C1–C2 and C5–C6 bonds.

Table IV. Intramolecular Bond Angles (deg) in 2

C1–Rh–C2	37.2 (5)	N2–Rh–C6	98.6 (5)
C5–Rh–C6	37.0 (5)	Rh–N1–C9	131 (1)
C1–Rh–C5	94.4 (6)	Rh–N1–C13	113.4 (9)
C2–Rh–C6	91.2 (7)	Rh–N2–C14	113 (1)
C1–Rh–C6	81.3 (6)	Rh–N2–C15	128.2 (9)
C2–Rh–C5	81.2 (7)	N1–C13–C14	113 (1)
C8–C1–C2	122 (2)	C13–C14–N2	121 (1)
C1–C2–C3	128 (2)	C9–N1–C13	116 (1)
C2–C3–C4	120 (1)	N1–C9–C10	125 (1)
C3–C4–C5	115 (1)	C9–C10–C11	118 (2)
C4–C5–C6	123 (1)	C10–C11–C12	115 (2)
C5–C6–C7	127 (1)	C11–C12–C13	126 (2)
C6–C7–C8	114 (1)	C12–C13–N1	121 (2)
C7–C8–C1	120 (1)	C12–C13–C14	126 (2)
Rh–C1–C8	108 (1)	C14–N2–C15	119 (1)
Rh–C1–C2	71.0 (7)	N2–C15–C16	116 (1)
Rh–C2–C3	109 (1)	N2–C15–H15	93 (6)
Rh–C2–C1	71.8 (7)	N2–C15–C17	109 (1)
Rh–C5–C4	112 (1)	C16–C15–H15	95 (7)
Rh–C5–C6	70.4 (9)	C16–C15–C17	109 (1)
Rh–C6–C7	114 (1)	C17–C15–H15	134 (6)
Rh–C6–C5	73 (1)	C15–C17–C18	117 (1)
N1–Rh–C1	92.0 (6)	C15–C17–C22	124 (1)
N1–Rh–C2	97.8 (7)	C18–C17–C22	119 (1)
N1–Rh–C5	167.5 (5)	C17–C18–C19	116 (2)
N1–Rh–C6	155.2 (5)	C18–C19–C20	124 (2)
N1–Rh–N2	79.3 (5)	C19–C20–C21	121 (2)
N2—Rh–C1	159.2 (5)	C20–C21–C22	121 (2)
N2–Rh–C2	162.2 (5)	C21–C22–C17	120 (1)
N2–Rh–C5	97.8 (5)		

structure was solved by the Patterson technique, and the position of the Rh atom was determined. All the remaining non-hydrogen atoms as well as the hydrogens of the pyridine ring, the methyl group, H14, and H15 were found from successive difference Fourier maps. The hydrogens of the cyclooctadiene and phenyl groups were theoretically calculated. Anisotropic refinement of all the non-hydrogen atoms except for the fluorines and isotropic refinement of the hydrogens (the phenyl and cyclooctadiene hydrogens being refined by using option AFIX 03 in SHELX) lead to the final agreement factors listed in Table I. No unusually high correlations were noted in the refinement. The atomic scattering factors for C, F, N, P, and Rh were computed from numerical Hartree–Fock wave functions,[27] and for hydrogen those of Stewart et al.[28] were used. Final positional and thermal parameters are listed in Table II. Bond lengths and angles are given in Tables III and IV based on these positions.

(27) Cromer, D. T.; Mann, J. B. *Acta Crystallogr., Sect. A: Cryst. Phys., Diffr., Theor. Gen. Crystallogr.* **1968**, *A24*, 321.
(28) Steward, R. F.; Davidson, E. R.; Simpson, W. T. *J. Chem. Phys.* **1965**, *42*, 3175.

Table V. Distances between Various Corresponding Atoms of Compounds 1 and 2 As Calculated by Program BMFIT[30]

atom		
compd 1	compd 2	dist, Å
Rh	Rh	0.021
N1	N1	0.017
N2	N2	0.016
C9	C9	0.264
C10	C10	0.716
C10	C11	0.842
C11	C12	0.259
C12	C13	0.100
C21	C14	0.048
H21	H14	0.250
cod	cod	0.26[a]

[a] The maximum observed distance between corresponding carbon atoms of the cyclooctadiene ligand.

The stereo drawings (Figures 1 and 2) were obtained by using Johnson's ORTEP2.[29] Figure 3 is a double stereo picture, drawn by using program BMFIT[30] which compares the structural characteristics of compounds 1 and 2. The plots were drawn by least-squares fitting of three common atoms (Rh, N1, and N2), and Table V lists distances between various corresponding atoms.

Determination of the Absolute Configuration of 2. When the refinement was completed, the test for determining the absolute configuration was carried out. Twelve reflections (table deposited as supplementary material) showed marked differences between $F_c(hkl)$ and $F_c(\bar{h}\bar{k}\bar{l})$ and were thus suitable for the Bijvoet test.[31] These reflections were measured. The structure was then further refined in its correct absolute configuration to the final agreement factors given in Table I. The coordinates given in Table II are those of the correct enantiomer with *S* configuration at C15.[32] This is a consequence of starting with (*S*)-1-phenylethylamine for the synthesis of NN″ = *N*-[(*S*)-1-phenylethyl]-2-pyridinecarbaldimine and $[Rh(cod)NN'']^+PF_6$ (2).

Comparison of the Rh Coordination in 1 and 2

Figure 1 gives a convenient stereoview of the molecule as well as the numbering system used in the crystallographic study. Figure 3 represents a double stereo picture comparing the structural characteristics of compounds 1 and 2.

As can be seen from Figure 3, the geometry around the Rh atom is almost identical for both compounds. However, there are some minor differences in the geometry of the cyclooctadiene moiety of the two complexes. Thus, whereas in compound 1 the four Rh–olefinic carbon distances are essentially identical (2.143 (6), 2.136 (5), 2.127 (6), and 2.125 (6) Å), in compound 2 two longer distances (2.18 (1) and 2.19 (1) Å and two undisturbed bonds (2.13 (1) and 2.10 (1) Å) were observed. Since the two Rh–N distances were found to be virtually identical (2.09 (1) Å), the observed lengthening of two of the Rh–olefinic carbon distances cannot be attributed to a "trans" effect. Contrary to what might be expected, the longer Rh–olefinic carbon bonds are associated with what appears to be a longer carbon–carbon distance (C1–C2 = 1.40 (2) Å) whereas the shorter C5–C6 bond of 1.34 (2) Å is related to the two shorter Rh–olefinic carbon distances. Thus, it seems that the somewhat asymmetric coordination of the cyclooctadiene ligand cannot be due to electronic effects but rather to steric hindrance between the pyridine and the

(29) Johnson, C. K. "ORTEP2", A Fortran Ellipsoid Plot Program for Crystal Structure Illustration, ORNL-5138, Oak Ridge, TN, 1972.
(30) Liu, L.-K. "Program BMFIT", University of Texas, Austin, 1977, based upon: Nyburg, S. C. *Acta Crystallogr., Sect. B: Struct. Crystallogr. Cryst. Chem.* **1974**, *B30*, 251.
(31) Bijvoet, J. M.; Peerdeman, A. F.; van Bommel, A. J. *Nature (London)* **1951**, *168*, 271.
(32) Cahn, R. S.; Ingold, C.; Prelog, V. *Angew. Chem.* **1966**, *78*, 423; *Angew. Chem., Int. Ed. Engl.* **1966**, *5*, 385.

Table VI. Parameters I–IX, Defining the Orientation of C*HMePh with Respect to the Rest of the Molecule in 1, 2, and 4[a]

parameter no.	numbering scheme of 2	general symbol	1[17]	2	4[27]
I	Mo–N2	M–N	2.119	2.086	2.182
II	N2–C15	N–C*	1.492	1.50	1.486
III	N1–Mo–N2	N′–M–N	78.9	79.3	74.0
IV	Mo–N2–C15	M–N–C*	128.9	128.2	123.4
V	N1–Mo–N2–C15	N′–M–N–C*	179.2	175.2	−172.7
VI	Mo–N2–C15–C17	M–N–C*–C(Ph)	−128.1	−73.5	−97.7
VII	Mo–N2–C15–C16	M–N–C*–C(Me)	104.5	162.2	135.3
VIII	Mo–N2–C15–H15	M–N–C*–H	−17.3	65.4	17.2
IX	N2–C15–C17–C22	N–C*–C_{ipso}–C_{ortho}[b]	77.6	−30.4	−62.1

[a] Distances in Å and angles in deg. [b] Nearest to N.

eight-membered ligand as exemplified by the following nonbonding intramolecular distances: C1–H9 = 2.55 Å, H1–H9 = 1.89 Å, C2–H9 = 2.67 Å, and H2–H9 = 2.12 Å. No similar short intramolecular distances were found between the cyclooctadiene ligand and the pyrrole ring in compound 1 (Figure 3).

The cyclooctadiene ligand seems to be somewhat better behaved in compound 1 (in terms of temperature factors and individual carbon–carbon distances) than in compound 2. This is not so surprising since a better refinement was attained for compound 1 (R = 0.031, R_w = 0.035) than that reached for compound 2 (R = 0.050, R_w = 0.046) and also because of the close proximity of the PF_6^- anion to the cyclooctadiene ring of compound 2 (see Figure 2). The pyridine ring is planar, and the maximum deviation of any atom from the least-squares plane defined by the six ring atoms is 0.04 Å.

Solid-State Orientation of the C*HMePh Substituent in 1, 2, and 4

Comparison of the structure of 2 with related molecules shows that the most interesting feature of its structure is the arrangement of the C*HMePh substituent with respect to the rhodium coordination sites, where during catalysis the prochiral substrates are bonded. A set of parameters I–IX has been defined to specify this orientation.[33] In the following discussion the cation of 2 is compared to the neutral Rh complex 1[17] in which the chelate ligand contains a pyrrole group instead of a pyridine group and to the cation of $[C_5H_5Mo(CO)_2NN'']PF_6^-$ (4)[34] which contains the same chelate ligand as 2.

In compounds 1, 2, and 4, the asymmetric substituent C*HMePh interacts with H14, referred to hereafter as the imine C proton. In addition, in the square-planar compounds 1 and 2 there is an interaction of C*HMePh with the neighboring part of the cyclooctadiene ligand and in the square-pyramidal compound 4 with the cyclopentadienyl and a carbonyl, these interactions differentiating 4 from 1 and 2.

The second column of Table VI lists parameters I–IX according to the numbering system employed for compound 2. In the third column these parameters are "translated" into general symbols, the values of which are presented in columns four–six for 1, 2, and 4, respectively.

Distances I and II show that the M–N bonds are shorter, whereas the N–C* bonds are slightly longer for the rhodium complexes 1 and 2 than for the Mo compound 4. Angle III is larger in the square-planar compounds 1 and 2 than in the square-pyramidal compound 4. Surprisingly, however, the M–N–C* angle IV is expanded in 1 and 2 compared to 4, thus increasing the interaction with the imine C–H bond. The torsional angle V, defining the deviation of C* from the plane of the chelate ring, shows that especially for compounds 1 and 2 atom C* is almost exactly in the ligand plane.

Scheme II. Newman Projections of Conformations a–d of Complexes 1–3 Looking along the N2–C15 Bond (Only Rear Part of the Complexes Shown)[a]

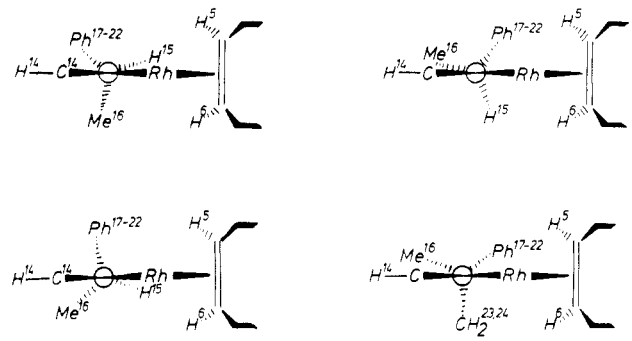

[a] The numbering system used refers to Scheme I (C* = C15).

The most important parameters are the torsional angles VI–VIII, describing the degree of rotation of the optically active substituent C*HMePh with respect to the M–N–C* plane. While 1 and 2 differ by about 60°, compound 4 is almost in the middle of them. For comparison with solution conformations, the arrangement of the C*HMePh substituents found in the solid state for 1 and 2 are shown in Scheme II. The drawings depict only the rear fragments of the complexes, illustrating by Newman projections intramolecular interactions along the N2–C*15 bond. The C14–H14 bond of the imino group in 2 almost eclipses C*–Me (conformation b), whereas in 1 it almost staggers the angle C*MePh (conformation a), 4 being intermediate (conformation c). The exact values of the torsional angles of the conformations a–c in Scheme II are given by gauges VI–VIII in Table VI.

An additional effect, contributing to the solid-state conformation of 2, seems to be a weak H15–F hydrogen bond to the PF_6^- anion. In the cation of 2 H15 is 0.86 Å below plane C (Table V) and pointing toward PF_6^- (H15–F5 = 2.42 Å; see Figure 2). In view of the well-documented existence of hydrogen bonding involving C–H groups and halogens[35] it is tempting to suggest that the conformational difference between compounds 1 and 2 is, at least partly, due to C–H···F hydrogen bond formation.

The torsional angle IX, N–C*–C_{ipso}–C_{ortho} (nearest to N), defines the phenyl orientation. In this respect 1 and 2 are very different, the two phenyls being almost perpendicular to each other.

(33) Bernal, I.; Ries, W.; Brunner, H.; Rastogi, D. K. J. Organomet. Chem. 1985, 290, 353.
(34) Bernal, I.; LaPlaca, S. J.; Korp, J.; Brunner, H.; Herrmann, W. A. Inorg. Chem. 1978, 17, 382.
(35) Green, R. D. "Hydrogen Bonding by C-H Groups"; Wiley: New York, 1974.
(36) Hull, W. E. "Aspect 2000 Application Note No. 1", Bruker Report 1978, 1, 4.

Table VII. Proton and Carbon Chemical Shifts and Selected Coupling Constants of 1[a]

H/C	$\delta(^1H)$ (300 K)	$\delta(^{13}C)$ (310 K)	$^1J_{C,H}$, Hz	$^1J_{C,Rh}$, Hz
1	4.54	80.44	~155	13.4
2	4.50	80.68	~155	11.6
3	2.4-1.8	31.80		
4		31.71		
5	3.81	77.53	~155	12.5
6	3.97	77.59	~155	13.0
7	2.4-1.8	30.77		
8		30.62		
9	6.49	134.24	177.5	
10	5.95	111.66	169.0	
12	6.42	117.47	169.0	
13		142.60		
14	7.74	162.42	163.0	
15	4.43	60.17	140.0	
16	1.57	22.43	127.4	
17		144.63		
18		129.32	160.5	
19	7.2	127.63	158.0	
20		127.88	161.0	

[a] Chemical shifts are δ values relative to the solvent acetone-d_6 ($\delta(^1H) \equiv 2.05$, $\delta(^{13}C) \equiv 29.80$) at all temperatures. Assignment of 1, 2, 5, 6, and 3, 4, 7, 8 tentative. Chemical shifts do not differ significantly between 310 and 243 K.

Solution Orientation of the C*HMePh Substituent in 1, 2, and 3

Solution Structure of 1. The solution structure of 1 was investigated by its ^1H and ^{13}C NMR spectra at temperatures between 213 and 310 K. The ^{13}C NMR spectrum of 1 (Table VII) shows eight distinct signals for the 1,5-cod carbons. The four carbons of the complexed double bonds have coordination shifts[24,25] of about −50 ppm, and each of these signals has a characteristic coupling to ^{103}Rh, which rules out any fast dissociation process between the metal and the cod ligand.

The ^1H NMR spectra are in agreement with the structural information derived from the carbon-13 spectra. In addition magnetization transfer experiments[22,23] indicate that in 1, at 300 K, there is a very slow exchange which leads to a pairwise coalescence of the olefinic proton signals. We interpret this as being due to a slow dissociation of the Rh–N(imine) bond, followed by rotation around the Rh–N(pyridine) bond (cf. the discussion of the solution structure of 2). This process is not observed when the spectra are recorded at 243 K (Figure 4).

The conformation of 1 was investigated by ^1H NMR nuclear Overhauser difference spectroscopy at 243 K in acetone-d_6 (concentration 10%). The normal 400-MHz spectrum of 1 is shown in trace A of Figure 4. The NOE difference spectra B–G in Figure 4 are given in stacked plot presentation, displaced to the right. The scale refers to spectrum A. The difference spectra are obtained by subtraction of a free induction decay, recorded after saturation of a signal from a free induction decay without saturation.[22,23] This technique leads to negative signals for the protons which are saturated and in general to positive signals for those protons for which there is dipole–dipole interaction through space.[37] Positive signals therefore are an indication of spacial vicinity to a proton that is saturated. All the other signals in this NOE difference spectroscopy average to zero.

(37) Noggle, J. H.; Schirmer, R. E. "The Nuclear Overhauser Effect", Academic Press: New York, 1971.

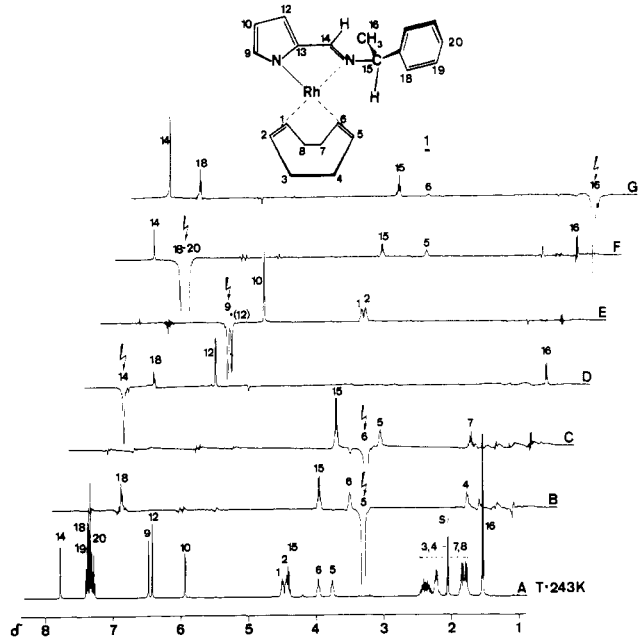

Figure 4. 400-MHz ^1H NMR spectra of 1 in acetone-d_6 at T = 243 K: (A) normal spectrum and (B–G) NOE difference spectra. The saturated signals are marked with arrows.

In spectrum B the olefinic proton 5 was saturated (arrow). As expected, the signals of the adjacent protons of the cod moiety, the olefinic proton 6 and the aliphatic protons 4, increase in intensity. Also, the signals of proton 15 at the asymmetric center and of ortho protons 18 of the phenyl ring are augmented. Therefore, the double bond C5=C6 must be cis to the imine N2 and both the substituents C*–H15 and C*–Ph have to be close to H5. In spectrum C, the signal of proton 6 of the double bond C5=C6 is saturated. Except for the neighboring cod protons, only the signal of H15 increases. There is no enhancement of the ortho phenyl protons 18, and the integrated intensity of the methyl signal 16 is zero. These two experiments are in agreement with a rotamer of structure c (Scheme II). Since the intensity enhancement of H15 is larger in spectrum B, H15 must be closer to H6 than to H5 and Ph is closer to H5 than Me to H6. In good agreement with conformation c there are increases of the signals of the Ph ortho protons and especially of the methyl protons 16 (besides 12) on saturation of the imine proton 14 in spectrum D.

Saturation of proton 9 in spectrum E increases the signal of the neighboring H10 of the pyrrole ring and also of H1 and H2 of the adjacent olefinic double bond, as expected. Since the NOE enhancements of 1 and 2 are similar, the assignment of these protons remains tentative. The assignment given in Figure 4 is based on magnetization transfer experiments at 300 K which may be interpreted by means of the dissociation of the Rh–N(imine) bond. In spectrum F, the ortho protons 18 of the phenyl ring are saturated. Besides proton 15 and methyl protons 16 of the optically active substituent, imine proton 14 and cod proton 5 signals increase in intensity. On saturation of the methyl protons 16, in spectrum G, the signals of 15 and 18 as well as the signals of 14 (strongly) and 6 (weakly) are augmented, demonstrating that methyl group 16 is in the position shown in conformation c of Scheme II.

Solution Structure of 2. Compound 2 dissolved in acetone-d_6 or tetrahydrofuran-d_8 exhibits dynamic proton and carbon-13 NMR spectra in the temperature range between 310 and 173 K (Table VIII). At 300 K only two olefinic carbons (protons) are observed for the cod ligand, whereas four signals can be detected below 210 K. Each

Table VIII. Proton and Carbon Chemical Shifts and Selected Coupling Constants of 2[a]

H/C	δ(¹H) (193 K)	δ(¹³C) (193 K)	$J_{C,H}$, Hz	$J_{C,Rh}$, Hz
1	4.69	87.09	~155	10.3
2	4.62	85.95	~155	9.5
3	2.5-1.8	30.94		
4		30.37		
5	4.14	85.33	~155	11.0
6	4.74	85.05	~155	7.9
7	2.5-1.8	~30.0		
8		~30.0		
9	8.12	150.35	183.1	
10	7.88	129.96	171.5	
11	8.36	129.65	172.5	
12	8.23	142.42	172.3	
13		156.10		
14	8.87	171.93	177.8	
15	4.96	63.81	143.6	
16	1.75	22.68	129.2	
17		141.35		
18		127.22	~160	
19	7.4	129.59	~162	
20		128.75	161.5	

[a] Chemical shifts are δ values relative to the solvent acetone-d_6 (δ(¹H) = 2.05, δ(¹³C) = 29.80) at all temperatures. Assignment of 1, 2, 5, 6 and 3, 4, 7, 8 tentative.

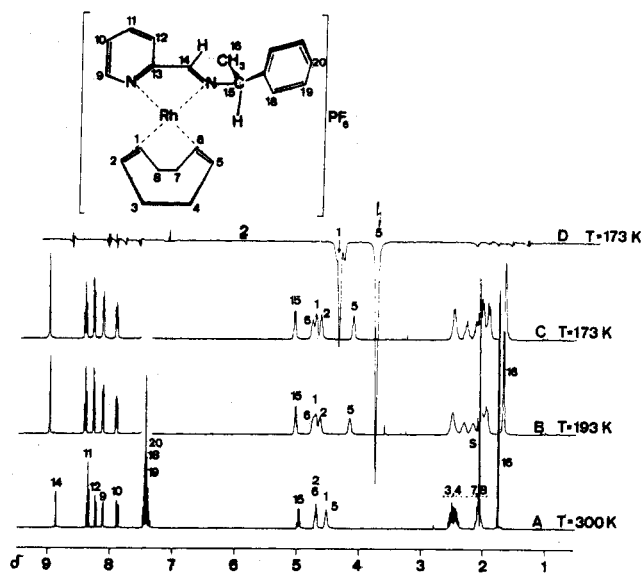

Figure 5. 400-MHz ¹H NMR spectra of 2 in acetone-d_6 at various temperatures. (D) is a difference spectrum indicating exchange of protons 1 and 5.

of these four carbon resonances shows Rh coupling which indicates that the Rh–carbon bonds remain intact. Even at 173 K there is a very slow exchange process which is illustrated by trace D of Figure 5. For example, saturation of olefinic proton 5 leads, in the difference spectrum, to negative signals at 1. This is direct evidence for the chemical exchange of these two surroundings. A dissociation of the Rh–N(imine) bond and subsequent 180° rotation about the intact Rh–N(pyridine) bond may account for this process, although other mechanisms cannot be excluded. The conclusion as to the preferred conformation of 2 in solution was reached from NOE experiments and comparison with 1. Overhauser effects in exchanging systems are difficult to interpret; however, in this case identical effects around the chiral center were found for both 1 and 2. Therefore, we conclude that the conformation of 2 must be similar to that of 1.

Table IX. Proton and Carbon Chemical Shifts and Selected Coupling Constants of 3[a]

H/C	δ(¹H) (300 K)	δ(¹³C) (310 K)	$J_{C,Rh}$, Hz
1	4.41	81.41	11.0
2	4.35	80.90	11.0
3	2.3-1.5	32.41	
4		31.67	
5	3.29	74.63	14.5
6	3.67	74.31	13.5
7	2.3-1.5	31.20	
8		30.79	
9	6.47	132.78	
10	5.99	111.37	
12	6.50	117.17	
13		142.24	
14	7.88	160.95	
15		67.18	
16	1.52	below solvent	
17		150.35	
18	7.45	128.92	
19	7.40	126.93	
20	7.29	127.36	
23/24	2.07	28.22	
	1.85		
25	0.89	9.03	

[a] Chemical shifts are δ values relative to the solvent acetone-d_6 (δ(¹H) ≡ 2.05, δ(¹³C) ≡ 29.80) at all temperatures. Assignment of 1, 2, 5, 6, and 3, 4, 7, 8, 16, 23, 24 tentative. Chemical shifts do not differ significantly between 310 and 243 K.

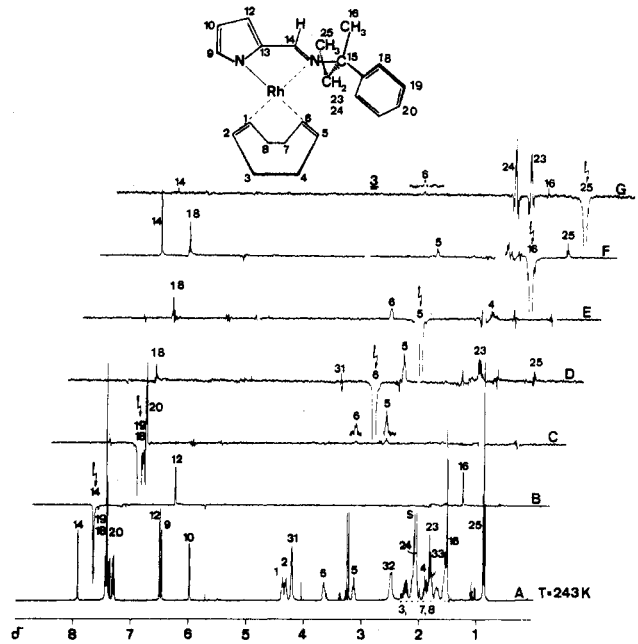

Figure 6. 400-MHz ¹H NMR spectra of 3 in acetone-d_6 at 243 K: (A) normal spectrum and (B–G) NOE difference spectra. For assignment see text and Table IX.

Solution Structure of 3. The carbon-13 spectrum of 3 at 243 K shows eight signals for the complexed cod ligand and 13 signals for the optically active ligand in agreement with its anticipated structure (Table IX). No attempts have been made to assign all the resonances of the sp^3 carbons 3, 4, 7, 8, 16, and 23 unambiguously. In addition, lines due to the byproduct $[(cod)RhCl]_2$ (signals 31 and 32 in Figure 6) can be identified. According to the ¹H NMR NOE spectra B–G (Figure 6), the preferred conformation of complex 3 at 243 K in acetone-d_6 solution is

d (Scheme II). The methyl group 16 of the chiral center is relatively close to the azomethine proton 14 (spectrum B), however, not in a completely eclipsed position but somewhat above the Rh plane on the side of cod proton 5. Besides the 14/16 interaction, spectrum B also shows a weak increase of the proton signals 23 and 24 of the ethyl group, but no increase of the ortho protons 18, in agreement with conformation d. Spectrum C demonstrates spacial proximity of the phenyl protons to cod protons 6 and especially 5. There is also a slight increase of the signals of methyls 16 and 24, but not of imine proton 14.

In spectra D and E the olefinic protons 6 and 5 were irradiated. In the case of 6, the signal increases for one of the diastereotopic protons 23, 24, and for the phenyl protons 18. In the case of 5, only the phenyl protons are enhanced in good agreement with conformation d. In addition, spectrum D indicates that there is still a very slow exchange of **3** with $[(cod)RhCl]_2$ (signals 31).

Saturation of methyl protons 16 increases 14 and 18 and very weakly 5 and 24 (spectrum F). The orientation of methyl group 25 of the ethyl substituent follows from spectrum G. Irradiation of 25 increases 23 and 24, as expected, and in addition 16, 6, and 14. Thus, in conformation d (Scheme II) methyl 25 must be located below the Rh plane close to the imine N2 on the side of cod proton 6, almost equidistant to the methyl protons 16, the imine proton 14, and the olefin proton 6. Irradiation of 9, 1, 2 (not shown in Figure 5) establishes the neighborhood of pyrrole protons 9 and 10 and cod protons 1 and 2.

Conclusion

The conformations of complexes **1–3** in the solid state and in solution have been determined by X-ray structure analyses and NOE difference spectroscopy. The rotation of the chiral substituent with respect to the Rh coordination plane is the only intramolecular motion open to compounds **1–3** able to change the shape of the molecules. In the crystal and in solution the phenyl ring of a C*HMePh or a C*MeEtPh substituent prefers not to eclipse bonds in the rhodium coordination plane and adopts a more or less perpendicular arrangement to that plane, sometimes being a littler close to the imine part in the chelate ring and sometimes to the adjacent cod double bond. A hydrogen substituent at the asymmetric center tends to orient toward the cod double bond in solution as well as in the solid state; it may deviate from that position by up to 60°. The methyl group of the asymmetric center usually is close to the imine system of the chelate ligand also in complex **3**, where the hydrogen is replaced by an ethyl substituent. In complex **1** there are only minor differences between solid-state conformation a and solution conformation c (Scheme II).

Acknowledgment. H.B., P.B., and G.R thank the Deutsche Forschungsgemeinschaft, the Fonds der Chemischen Industrie, and the BASF AG for support of this work. I.B. and G.M.R. thank the U.S. National Science Foundation for providing funds to purchase the diffractometer, the Robert A. Welch Foundation for research support (Grant E-594), and the Computer Center of the University of Houston for a generous supply of free computing time.

Supplementary Material Available: A table of atomic coordinates and thermal parameters for complex **2** including the hydrogen atoms and tables of the determination of absolute configuration, least-squares planes and atomic deviations, and structure factors for complex **2** (14 pages). Ordering information is given on any current masthead page.

Rapid, Reversible Ortho Metalation in $RuHCl[P(C_6H_5)_3]_3$ and Its Role in the Catalytic Hydrogenation of Alkynes

Alan M. Stolzenberg*[1a,b] and Earl L. Muetterties[1a,2]

Departments of Chemistry, University of California, Berkeley, California 94720, and Brandeis University, Waltham, Massachusetts 02254

Received December 12, 1984

Reaction of $RuHCl[P(C_6H_5)_3]_3$, **1**, and alkynes produces the ortho-metalated complex $RuCl[P(C_6H_4)(C_6H_5)_2][P(C_6H_5)_3]_2$, **3**, which is present during catalytic alkyne hydrogenation reactions. **3** is converted to **1** by reaction with H_2. The $^2H\{^1H\}$ NMR spectrum of **1**-d_2 produced by reaction of D_2 and **3** establishes rapid, reversible, intramolecular hydrogen isotope exchange between hydride and ortho-aryl phosphine sites, with deuterium preferred in the latter sites. The exchange and position of equilibrium result in an apparently slow rate of intermolecular exchange between D_2 and the hydride site. Examination of hydrogen isotope exchange during alkyne hydrogenation establishes that **3** is not an intermediate in the hydrogenation reaction.

Introduction

Intramolecular C–H activation in transition-metal phosphine and phosphite complexes has been of interest for a considerable time period.[3] The impression one garners from the existing literature is that intramolecular C–H activation is relatively slow.[4,5] As a consequence, it generally has not been regarded as a potential fundamental step in the mechanisms of reactions catalyzed by these

(1) (a) University of California. (b) Brandeis University (present address).
(2) Deceased January 12, 1984.
(3) Parshall, G. W. *Acc. Chem. Res.* **1970**, *3*, 139.
(4) Parshall, G. W.; Knoth, W. H.; Schunn, R. A. *J. Am. Chem. Soc.* **1969**, *91*, 4990–4995.
(5) James, B. R.; Markham, L. D.; Wang, D. K. W. *J. Chem. Soc., Chem. Commun.* **1974**, 439–440.

0276-7333/85/2304-1739$01.50/0